ISSN: 2634 - 8853

Journal of Engineering and Applied Sciences Technology

SCIENTIFIC Research and Community

Research Article

Open Access

Graphitic Carbon Nitride (g-C_3N_4)/ZnO Perovskite-Based Interface for Sustainable Decontamination of Pollutants from Wastewater Using Visible-Light Driven Photo-Catalysis

Sahima Tabasum[1]* and Sadhia Tabassum[2]

[1]Department of Environmental Sciences, School of Climate Change and Sustainability, Institution of Eminence, University of Delhi, Delhi, India

[2]Department of Environmental Science, School of Chemical Engineering and Physical Sciences, Baba Ghulam Shah Badshah University, Rajouri, Jammu and Kashmir, India

ABSTRACT

The rapid advancement of industrial and agricultural activities has led to an escalation of pollution, with organic pollutants, particularly pesticides, being directly discharged into water bodies. This contamination poses serious environmental and health challenges. Among these pollutants, carbofuran, a widely used pesticide, significantly threatens aquatic ecosystems and human life. To address this issue, innovative approaches are essential to mitigate the adverse effects of carbofuran. Nanocomposites have become promising materials for photocatalytic degradation of organic and inorganic pollutants due to their exceptional physicochemical properties, cost-effectiveness, and high stability. Graphitic carbon nitride, a polymeric material composed of carbon, nitrogen, and trace impurities, is gaining considerable attention for photocatalysis due to its unique semiconducting characteristics and catalytic activity.

Recent studies reveal that doping g-C_3N_4 has high photocatalytic performance under visible light. g-C_3N_4 exhibits superior catalytic efficiency, facilitating the mineralization of Atrazine in aqueous environments. This improved activity is attributed to the synergistic effects of the dopants, which optimize the electronic structure of g-C_3N_4. The advancement of g-C_3N_4-based nanocomposites offers a promising pathway for the development of effective and sustainable solutions to tackle water pollution and safeguard environmental health.

The nanocomposite is synthesized using hydrothermal and microwave techniques. The powder X- ray diffraction technique is employed to identify the crystal structure of a ternary nanocomposite material, specifically focusing on the crystallite size, phase, and defects. The surface morphologies and functional groups are assessed using SEM and Fourier-transform infrared spectroscopy (FTIR). The FTIR analysis reveals the presence of C–N and C=N stretching modes in the heterocycle, characterized by bands ranging from 1200 to 1650 cm^{-1}. The experiment aimed to study the effects of several experimental factors, including pH, time, and Catalyst Dose, on the breakdown of Atrazine.

***Corresponding author**

Sahima Tabasum, Department of Environmental Sciences, School of Climate Change and Sustainability, Institution of Eminence, University of Delhi, Delhi, India.

Received: January 04, 2025; **Accepted:** January 06, 2025; **Published:** January 18, 2025

Keywords: Pollution, Water Treatment, Nanomaterials, Mineralization

Introduction

The agricultural sector is an indispensable fundamental of economies, both in developed and developing countries [1,2]. However due to pest, insect, and weed damage there have been serious losses incurred as many of the farmers are left with crop yields lower than expected [3]. Different pesticides are widely used as plant protection agents to protect crops improve their yield and protect their quality [4,5]. Of these, the most frequent chemical groups are organochlorine, organophosphate, and carbamate pesticides. These pesticides and their degradation products are transported by agricultural runoff to water bodies including streams, rivers, and ponds [6].

Metabolic disorders and endocrine dysfunctions associated with embryonic death have been well- cited for pesticides from these chemical classes [7]. The carbamate contamination of water leads to negative consequences on aquatic animals. Here, on the other hand, action needs to be taken to reduce and minimize the pollution from agriculture and industrial effluents from killing our aquatic systems. Because of its long-term benefits of stability, efficiency, greenness, and sunlight direct use as the driving force, photocatalytic technology has attracted focus for nearly 40 years in the research field of solar energy semiconductors. Graphitic carbon nitride g-C_3N_4, a two-dimensional non-metallic and semiconducting polymer, has an ultra-small band gap enabling its function in the visible region. Which was synthesized based on a simple thermal polycondensation method. Another feature of g-C_3N_4 is that it is an exceptionally effective visible-light photocatalyst with very little toxicity and appropriate band

positions. Atrazine is a human-made pesticide used to control weeds in agricultural areas, forestry, and non-crop areas. Broadleaf and grassy weeds are prevented and controlled by atrazine in plantations of eucalypts, soybeans, corn, sugarcane, sorghum, lupins, and pine. Additionally, grass surfaces like home lawns and golf courses employ it.

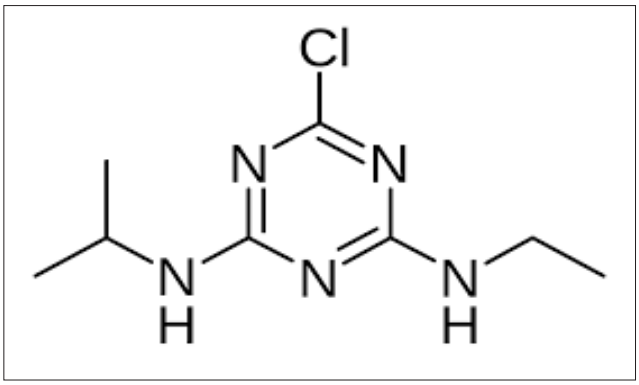

Figure 1: Structure of Atrazine (2-chloro-4-ethylamino-6-isopropylamino-1,3,5-triazine)

Materials and Method

Thiourea (99%), ethanol, sodium hydroxide, Zinc nitrate, Aloe Vera, hydrogen peroxide, hydrochloric acid, cesium bromide (CsBr), bismuth tribromide, and DI water. All chemicals are analytical grade and used without additional refinement.

Synthesis of g-C_3N_4 Nanocomposites

For making g-C_3N_4 Thiourea was heated in a ceramic crucible covered with a lid, and placed in a muffle furnace at 600º C for two hours at a thermal heating rate of 5º C/min to create g-C_3N_4. The crucible was taken out of the muffle furnace and cooled down at room temperature before being crushed in an agate mortar into a fine yellow powder [8].

Synthesis of g-C_3N_4/ZnO Nanocomposites

ZnO was synthesized using an eco-friendly method employing Aloe Vera gel and deionized (DI) water. Zinc nitrate (9.40 g) was added to the solution and stirred for 120 minutes, followed by a 12-hour resting period. Subsequently, 0.30 g of g-C_3N_4 powder was added slowly to the resultant mixture and stirred for 1.5 hours to prepare the g-C_3N_4/ZnO nanocomposite as shown in Figure 2. The resulting light yellow-colored precipitates were washed with water and ethanol and then calcined at 220 °C.

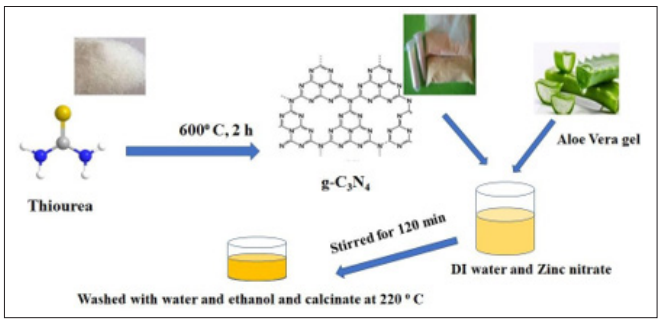

Figure 2: Preparation the g-C_3N_4/ZnO Nanocomposite

Synthesis of g-C_3N_4/ZnO/Perovskite Nanocomposites

For the synthesis of $Cs_3Bi_2Br_9$ nanoparticles, a facile physical mixed method was used. In this approach, cesium bromide (CsBr) and bismuth tribromide ($BiBr_3$) were meticulously ground together using a mortar and pestle to achieve intimate mixing at the molecular level. The Solution was subsequently exposed to thermal treatment at 600 °C for 4 hours in a muffle furnace. This high-temperature annealing process facilitated the solid-state reaction between the precursors, leading to the formation of crystalline $Cs_3Bi_2Br_9$ nanoparticles

Photo-Catalytic Activity Tests

When exposed to visible light, atrazine at a concentration of 100 mg/L was broken down to measure the photocatalytic activity. A appropriate batch reactor with a visible light source was used to conduct photocatalytic activities. 10 mg of the nanocomposite was added to 30 mL of atrazine solution for the photocatalytic test, and 0.1 M HCL and NaOH were used to maintain a steady pH. The solution was left at room temperature and exposed to visible light prior to the start of the reaction. The solutions were centrifuged and filtered using Whatman (0.45 mm) filter paper at predetermined intervals in order to remove the nanocomposite. The filtrates were then examined at 222 nm using a UV-Vis spectrophotometer [6,9]. The effects of various experimental conditions, particularly pH and time, on Atrazine elimination were examined. The proportion of photocatalytic pesticide degradation was calculated using the equation below:

Percent Degradation = $AO-At\ /AO$ ×100

Where AO is the absorbance of pesticides at the initial stage, and at, is the absorbance of pesticides at a time "t".

Operating Parameter Effect

A wide range of operational parameters influences the photocatalytic breakdown rate of organic pollutants or pesticides in the aqueous phase. This study investigated pH, irradiation time, and other variables. These factors were studied one by one to examine how they impact the catalytic efficiency of the synthesized composite material in insecticide.

pH Effect on Photocatalytic activity

The effects of pH on the rate of photocatalytic degradation of Atrazine were investigated at various pH levels. Each time, pH was maintained with 1M HCl or 1M NaOH and measured using a pH meter.

Effect of Photocatalyst Dose

The photocatalyst's optimal mass must be calculated in order to avoid overuse within the system. To that end, the effect of photocatalyst dosage on the breakdown of Atrazine insecticides was purposefully examined by increasing photocatalyst quantity from 0.01 to 0.06 g/L while maintaining other parameters constant.

Effect of Irradiation

Time In this study, an Atrazine solution containing a synthetic nanocomposite was exposed to UV light at different time intervals while all other variables remained constant, and the findings were recorded.

Result and Discussion

Characterization of Material

The picture presents an illustration of the FTIR spectra of each of the photocatalyst compounds. The broad peaks at 3000-3500 cm-1 indicate the presence of O-H stretching vibrations, likely associated with adsorbed water molecules on the surface of the materials. The Sharp Peaks at 1630-1650 cm-1 are attributed to the C=N stretching vibrations, characteristic of the triazine ring in g-C_3N_4. Peaks at 1300-1500 cm-1 are assigned to C-N stretching vibrations

in the triazine ring and C-NH bending vibrations, confirming the presence of g-C_3N_4. Peaks at 500-800 cm-1 are characteristic of Zn-O stretching vibrations, indicating the presence of ZnO in the nanocomposite as shown in Figure 3. The additional peaks observed in the g-C_3N_4/ZnO/perovskite spectrum likely correspond to the perovskite component, suggesting its successful integration into the nanocomposite structure.

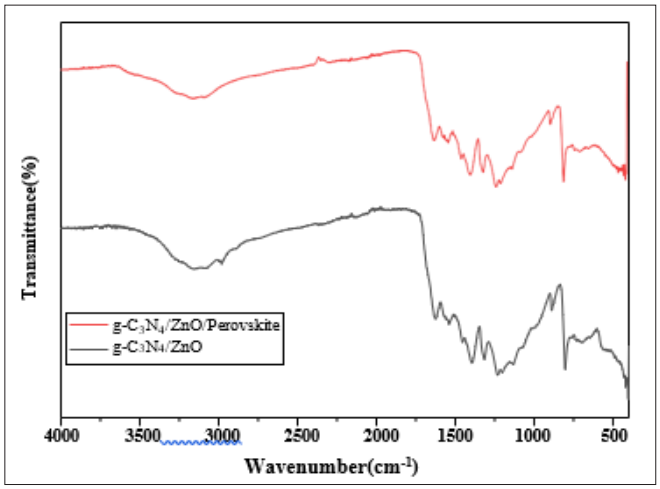

Figure 3: FTIR pattern of g-C_3N_4/ZnO, and g-C_3N_4/ZnO/perovskite nanocomposite

Ray Diffraction Analysis

Through X-ray diffraction, the crystallinity of each nanomaterial was identified. The produced material's is crystalline phase as determined by X-ray diffraction. The hexagonal phase of the g-C_3N_4 was formed, as indicated by peaks at 13º and 27.5º, which correspond to crystallographic planes (100) and (002), respectively [JCPDS FILE NO.87-1526]. For g-C_3N_4/GO, a peak of graphene oxide at 10.8º corresponds to the (001) plane.

Photocatalytic Activity

Degradation Efficiency of Synthesized Photocatalyst

pH Effect

The findings of a research study are depicted in Figure 4(a), which shows the influence of pH on the photodegradation of Atrazine by all photocatalyst materials when the substances were exposed to visible light. The efficiency of Atrazine removal increased with an increasing pH range of 6.0 to 7.0 but reduced as the pH was elevated further from 7.0 to 10. This phenomenon was observed across all photocatalysts. The perfect pH value, which was 6.0, was found to have maximum Atrazine removal efficiencies of 70.12, and 89.3% with g-C_3N_4/ZnO, and g-C_3N_4/ZnO/Perosvkite photocatalytic nanocomposite, in the visible region. The photocatalyst's surface charge contributes significantly to removing Atrazine from the environment. When exposed to a pH 6, the surfaces of all photocatalysts become predominantly positively charged, which leads them to rebuff cationic moiety electrostatically. When the pH of the environment is alkaline (more than 7.5), the electrostatic repulsion towards anionic compounds is predominant [7]. This causes all photocatalyst nanomaterials surfaces to become negatively charged. Using the g-C_3N_4/ZnO/Perosvkite nanocomposite removed the greatest amount of Atrazine. It is also possible that OH-/H_2O and localized holes participated in an electron transfer reaction, which resulted in the production of a high number of hydroxyl radicals that sped up the decomposition of Atrazine when it was exposed to visible light.

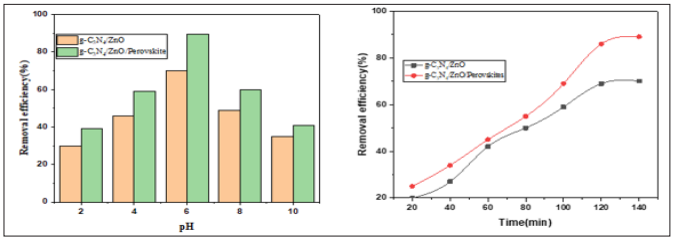

Figure 4: Degradation of Atrazine pesticide (a) pH (b)time study

Kinetics

The effect of contact (irradiation) is seen as elimination efficiency rose as the irradiation time increased. Extending the irradiation time interval from 20 minutes to 120 minutes resulted in an increase in the percentage of degradation from 19 to 70.12% and 20.25 to 89.3% using g-C_3N_4/ZnO, and g-C_3N_4/ZnO/Perosvkite for the nanocomposite. This may be attributed to the fact that as the irradiation period increases, the Atrazine molecules have more time to react with the surface of the catalyst and create hydroxyl radicals. This speeds up the photocatalytic process, which in turn raises the percentage of Atrazine that has been degraded.

Effect of Photocatalyst Dose

To determine the optimal photocatalytic dosage, the amounts of the g-C_3N_4/ZnO, g-C_3N_4/ZnO/Perosvkite, nanocomposites were varied from 0.1 to 0.5 g/l in 100 ml of Atrazine solution and 100 w intensity at pH 6.0 for up to 2 hours. When the dose of the photocatalyst was increased from 0.1 to 0.3 g/l, the photocatalytic removal efficiency of Atrazine increased from 70.12% to 89.3%. However, increasing the dose beyond 0.3 g/l did not have any effect on the efficiency of the elimination process.

Desorption/Regeneration Studies

Experiments on desorption were carried out in order to ascertain whether or not photocatalyst regeneration is even possible. As a desorbing agent, 0.1 M HCL was utilized to research the desorption of contaminants from the surface of the nanocomposite. In a nutshell, 0.1 g of used nanocomposite material was added to a beaker, and the mixture was agitated for a total of 2 hours.

After that, the pollutant-loaded adsorbent was centrifuged to separate it from the pollutants, and the residual concentration was measured.

Following the adsorption being carefully cleaned with DI water to remove any adsorbed molecules that may have been present on the surface of the adsorbent, it was then air dried so that it could be used in subsequent cycles. The equation allowed for the determination of desorption efficiency.

$$D\% = \left(\frac{q1,desorption}{q2,adsorption}\right) \times 100$$

The efficiency of Atrazine removal peaked at 44% in the fifth cycle and then gradually decreased

Conclusion

To successfully produce a g-C_3N_4/ZnO, and g-C_3N_4/ZnO/Perosvkite nanocomposite, a straightforward and cost-effective method was methodically utilized. The ternary g-C_3N_4/ZnO/Perosvkite photocatalyst outperformed the other photocatalyst [7,10]. The ideal pH value, which was found to be 6.0, was found to have maximum Atrazine removal efficiencies of 70.12, and 89.3% with g-C_3N_4/ZnO, g-C_3N_4/ZnO/Perosvkite. The research

found that improving Atrazine breakdown required increasing the catalyst dosage to 0.3 g/l for the best results [11].

References

1. Larsen AE, Claire Powers L, McComb S (2021) Identifying and characterizing pesticide use on 9,000 fields of organic agriculture. Nature Communications 12: 5461.
2. Möhring N, Dalhaus T, Enjolras G, Finger R (2020) Crop insurance and pesticide use in European agriculture. Agricultural Systems 184: 102902.
3. Tudi M, Daniel Ruan H, Wang L, Lyu J, Sadler R, et al. (2021) Agriculture development, pesticide application, and its impact on the environment. International journal of environmental research and public health 18: 1112.
4. Miah SJ, Hoque A, Paul A, Rahman A (2014) Unsafe use of pesticide and its impact on the health of farmers: a case study in Burichong Upazila, Bangladesh. cancer 21: 22-30.
5. Zhang J, Wang J, Zhou X (2019) Farm machine use and pesticide expenditure in maize production: health and environment implications. International Journal of Environmental Research and Public Health 16: 1808.
6. Wang J, Wang S (2022) A critical review on graphitic carbon nitride ($g\text{-}C_3N_4$)-based materials: Preparation, modification and environmental application. Coordination Chemistry Reviews 453: 214338.
7. Tabasum S, Sharma A, Rani S, Chaudhary S, Malik AQ, et al. (2023) Prolific Fabrication of Lanthanum Oxide with Graphitic Carbon/Graphene Oxide for Enhancing Photocatalytic Degradation of Carbofuran from Aqueous Solution. Rasayan Journal of Chemistry 16.
8. Olisah C, Okoh OO, Okoh AI (2020) Occurrence of organochlorine pesticide residues in biological and environmental matrices in Africa: A two-decade review. Heliyon 6: e03518.
9. do Rego EL, Nakamura TC, Diniz PHGD, Oliveira UR, de Souza JR, et al. (2022) Spatiotemporal evaluation of organochlorine pesticide residues in bottom sediments of the Rio de Ondas hydrographic basin, western Bahia, Brazil. Environmental Science and Pollution Research 29: 50376-50391.
10. Jiang XY, Kwon E, Chang HC, Huy NN, Duan X, et al. (2023) Tuning nanostructured $CuCo_2O_4$ on 3D macro-support for enhanced degradation of carbofuran via catalytic activation monopersulfate: Key roles of morphology and active species. Separation and Purification Technology 308: 122789.
11. Wanjiku Philip S, Madadi Odongo V, Wandiga SO, Omayio DG, Okumu MO (2022) Estimation and human health risk assessment of organochlorine and organophosphate pesticide residues in raw milk collected in Kenya. F1000Research 11: 14.